Meccanica (2024) 59:1327–1334
https://doi.org/10.1007/s11012-024-01860-9

RESEARCH

A new combined fabrication process to shape small flexure hinges

Marco Fava · Vincenzo Parenti-Castelli · Michele Conconi · Nicola Sancisi

Received: 28 March 2024 / Accepted: 16 July 2024 / Published online: 27 July 2024
© The Author(s) 2024

Abstract This paper presents a new combined fabrication method, named 3D-PLAST, aimed at overcoming inherent limitations of conventional additive manufacturing techniques when producing small flexure hinges in compliant mechanisms. Flexure hinges play a crucial role in various applications, offering advantages such as cost reduction, increased precision, and weight reduction. However, traditional additive manufacturing proves challenging in achieving satisfactory mechanical properties when manufacturing small-size hinges. To overcome these limitations, the 3D-PLAST process combines fused filament fabrication with compressive plastic deformation. This hybrid process exploits the advantages of both techniques, i.e., flexibility, low cost, and ease of use. This process enables the fabrication of small-size mechanisms with good dimensional accuracy. Finally, the paper reports experimental tests on two materials comparing flexure hinges manufactured by 3D-PLAST versus 3D printing methods to demonstrate the effectiveness of the proposed process.

Keywords Flexure hinges · Additive manufacturing · Plastic deformation · Compressive forming · Bending endurance

M. Fava (✉) · V. Parenti-Castelli · M. Conconi · N. Sancisi (✉)
DIN-Department of Industrial Engineering, University of Bologna, Viale del Risorgimento 2, 40136 Bologna, BO, Italy
e-mail: marco.fava6@unibo.it

N. Sancisi
e-mail: nicola.sancisi@unibo.it

V. Parenti-Castelli
e-mail: vincenzo.parenti@unibo.it

M. Conconi
e-mail: michele.conconi@unibo.it

1 Introduction

A flexure hinge (FH), also known as a compliant joint, is the flexible part of a structure, which exhibits a lower stiffness in some specific positions and is exposed to more significant deformations than the rigid part when the structure is subjected to a force or a displacement. Compliant joints are applied in various fields, such as automobile, aviation, biomedical, medical devices [1], MEMS, and also musical instruments [2].

In [3], FHs are categorized into three classes, namely single-, double- and multiple-axis hinges. Single-axis ones are used in planar motion mechanisms, while all classes are used in spatial mechanisms. FHs can also be classified as symmetric or non-symmetric and, in general, can exhibit different notch shapes: circular, elliptical, parabolic, hyperbolic, and filleted V-shapes are some examples. Many papers have studied and modelled their behaviour to characterize their mechanical performances, such as deformation and stress vs applied forces [4, 5].

FHs can be stand-alone components inserted into a mechanism instead of traditional pairs. They can also be made from a single monolithic block of the mechanism, reducing its size and concentrating a high elasticity in narrow regions. In any case, a compliant mechanism is obtained with a behavior similar to that with traditional kinematic pairs, at least in a neighbourhood of a mechanism configuration.

The advantages of compliant monolithic mechanisms are many [6]: cost reduction, due to lower mechanism assembly costs and time, and to a simplification of production procedures, which do not require the creation of many parts; increased performances, due to weight reduction and increased precision. For these advantages, compliant mechanisms are often used in disposable surgical tools, which are cheaper than traditional ones based on rigid links and kinematic pairs. Indeed, disposable tools are easier and cheaper to manufacture, do not require sterilization for re-usability, and, remarkably, they may provide comparable dexterity.

FHs are usually manufactured via multi-material moulding [7], micro electro discharge machining [8], waterjet cutting, wire erosion, micro-milling [9], compressive plastic deformation [10], and additive manufacturing (AM) [11–15]. Among these, specifically when dealing with resins and plastic materials, AM is the most used, feasible, and less expensive method, also called 3D printing technique. AM is further classified based on the technology employed to create 3D structures, including techniques such as material extrusion, powder bed fusion [16], VAT photopolymerization, material jetting, binder jetting, sheet lamination, directed energy deposition, and more [17]. They all consist of adding material in a layer-by-layer approach. The difference lies in how they melt or deposit the layer, for example, by melting a filament and placing it in a certain path or by sintering a layer of powder with a laser and moving on to the next one.

This work mainly focuses on AM with fused filament fabrication (FFF), a widely used method since it involves low-cost printers and relatively cheap plastic materials such as polymers, nylon, or composite materials, which are frequently used in many applications. The main advantages of this process are: i) to allow the designer to generate complex geometries without the need for specific fabrication skills and knowledge of demanding procedures, and ii) to avoid cost overruns to recreate the desired elaborated geometry [18].

On the other hand, there are also limitations. As described in [19], the Ishikawa diagrams show how 3D object geometrical accuracy depends on several factors, such as pre-processing, human decisions, and activities. Moreover, FHs may be printed with different orientations of the material deposition filament with respect to the object to print. This may affect the final mechanical properties [20, 21]. The influence of orientation is negligible for FHs with relatively large notch sizes with respect to the filament size but becomes relevant when notch and filament sizes are comparable. In that case, FHs may not be printed correctly since, during the slicing phase, the software cannot correctly interpret such small dimensions. As a result, small sections may be skipped, the deposited material may be insufficient, or the joint may be welded together with other parts. Also, for "small" FHs, even when geometrically realised, the result could be a hinge with poor mechanical properties. The geometric accuracy of the hinge is also severely compromised, contributing to a worsening of its mechanical characteristics.

The designer may adopt the most favourable printing orientation, but this is possible when all FHs of the mechanism have the same orientation. However, when dealing with a spatial mechanism, it is practically inevitable that the optimal orientation for some flexure hinges will not be optimal for others. Thus, the result is a compliant mechanism with nominally identical hinges that are different in practice and with different mechanical characteristics. Consequently, this phenomenon becomes particularly negative for small mechanisms and small FHs.

A new manufacturing process is proposed here to overcome these limitations. It makes use of traditional 3D printing in combination with plastic deformation to obtain the notch of the FH. The technique is not affected by the size of the notch nor significantly by the deposition orientation of the print filament, and it is inherently simple and inexpensive. The new process consists of two phases. In the first phase, the system's whole "rigid" part is realized by 3D printing, leaving the material in the areas where the FH notch will be made. In the second phase, the FH notch is made by plastic deformation of the material. As a final result, a compliant mechanism with FHs is obtained with better properties than those obtained by

manufacturing the notch by 3D printing. In addition, the proposed process solves the problem of manufacturing small FHs while keeping low costs.

In this paper, the new combined process, named 3D-PLAST in the following, is studied and its advantages and limitations are shown. The mechanical characteristics of FHs made with standard FFF methods and the new 3D-PLAST process are compared using different materials and orientations. Finally, to show the potential of the proposed process, a prototype of a 4 mm diameter Cardan joint with hollow shafts is realised and presented.

2 Description and validation of the new combined manufacturing process

This section presents the new fabrication process, 3D-PLAST, followed by a description of the specimens produced, the materials, and the 3D printer setup. Finally, the adopted forming device and the specimens' manufacturing and testing procedures to validate the process are described.

2.1 3D-PLAST process

As mentioned above, the 3D-PLAST process combines two basic fabrication processes: additive manufacturing via FFF and cold compressive plastic deformation. The former is used to fabricate objects with printable dimensions, while the latter is applied to obtain a compressive plastic deformation to achieve the notch's shape and final thin size. More details are given in the subsequent sections.

2.2 Specimen characteristics

The process described in Sect. 2.1 is obviously conditioned by the mechanical characteristic of the material, and in particular by the compression yield strengh, that must be lower than the one reached through the plastic deformation process. The FH shape instead, may vary and it does not influence the procedure. The size of the crosspiece depends on the size of the final object and the printing limits of the 3D printer used, in this case a Mark Two 3D printer (Markforged, Watertown, MA, USA) with a nominal resolution of 0.1−0.2 mm. In this study two materials were adopted to create the specimens: Onyx and Nylon White, both compatible with the used 3D printer. Onyx is a black filament, a nylon (polyamide 6) filled with approximately 10% to 20% by volume of short carbon fibres [22]; Nylon White is an unfilled thermoplastic and non-abrasive material. Their mechanical characteristics change if the printing direction of the object is different [23].

With reference to Fig. 1b a Cartesian system (X, Y, Z), fixed to the specimen with origin at the midpoint O of the specimen size has been chosen. To take into account the influence of the printing directions two of them were chosen, namely along the Z and the Y axes, hereafter referred to as mode 1 and mode 2, respectively. Their mechanical properties are reported in Table 1, where E is the Young's modulus, ν is the Poisson's coefficient and σ_{yield} the compression yield stress.

The characteristics were taken from [23], where specimens with standard characteristics and geometries were produced by 3D printing (with the same 3D printer used in this study) and tested with standard procedures in both tension and compression. The yield strength σ_{yield} takes into account also the inhomogeneity of the specimens.

The Mark Two 3D printer has some limitations in the production of FHs with 0.5 mm crosspiece, so the new production process proposed in this paper can be used to achieve this crosspiece size. The 3D-PLAST process first makes the rigid part of the FH with printable dimensions and then deforms it by a plastic deformation process to create the shape of the FH. With reference to Fig. 1b the starting shape of the selected FH is a prism with cross section (y × z) 1.2 mm × 0.5 mm = 0.6 mm^2 and length 40 mm along the X-axis. Then, the plastic deformation is performed at the midpoint O of the specimen size in the X-axis direction. The shape of the FH was V-shaped, symmetrical, with an angle at the vertex of 90° and a radius at the vertex of 0.2 mm, with a crosspiece size of 0.5 mm. This type of shape was chosen because it

Table 1 Mechanical properties of materials

Material	E [GPa]	ν	σ_{yield} [MPa]	Mode
Nylon white	1.53 ± 0.11	0.27 ± 0.04	70	1
Nylon white	1.43 ± 0.08	0.26 ± 0.06	70	2
Onyx	0.57 ± 0.11	0.22 ± 0.01	75	1
Onyx	1.13 ± 0.12	0.38 ± 0.02	75	2

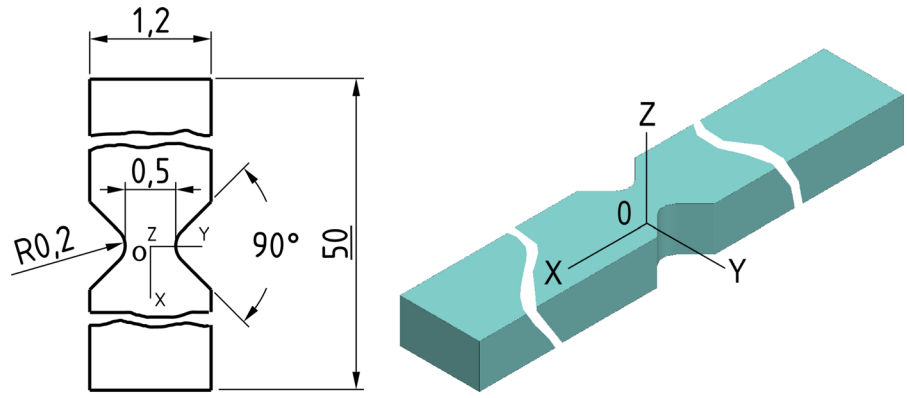

Fig. 1 3D specimen for FH: **a** geometry of the FH specimen; **b** CAD representation of the FH specimen

was hypothesized that punches would be more effectively produced with these geometries compared to others. However, this does not limit the use of this method for the production of other compliant shapes.

2.3 Punches

Two specular steel punches (1 and 2 in Fig. 2b) were used to form the desired shape of the FHs by the 3D-PLAST process. The two punches have a prismatic shape shown in Fig. 2 (all sizes are in millimeters). Their active parts, namely the edges that deform the specimen, have a symmetrical V-shape of 90° with a fillet radius at the vertex of 0.2 mm, such as to achieve the desired FH shape by plastic deformation.

Figure 2b represents the two punches seen under x47.8 microscope magnification. They are inserted into a specifically designed device, with the specimen interposed between them. The punches are guided to move in a direction orthogonal to the long axis of the specimen (Y direction, Fig. 1) until the desired crosspiece thickness is reached.

2.4 Equipment for the plastic deformation process

Figure 3 shows the punching device that allows the FH to be shaped by plastic deformation. The two punches (1 and 2) are connected to a prismatic slider (8) in a specular way with direction along the Y-axis of the specimen (6) and with the active edges perpendicular to the horizontal plane and can move one against the other. The upper parts of the two punch edges tighten the specimen to form the FH, which is freely supported by planar elements until they come into contact with the lamina (5) with their lower parts not occupied by the specimen. The thickness of the lamina equals that of the FH's crosspiece. In this way, the desired size of the FH crosspiece is precisely determined.

The two punches with the specimen interposed are pressed against each other by an external clamp (not

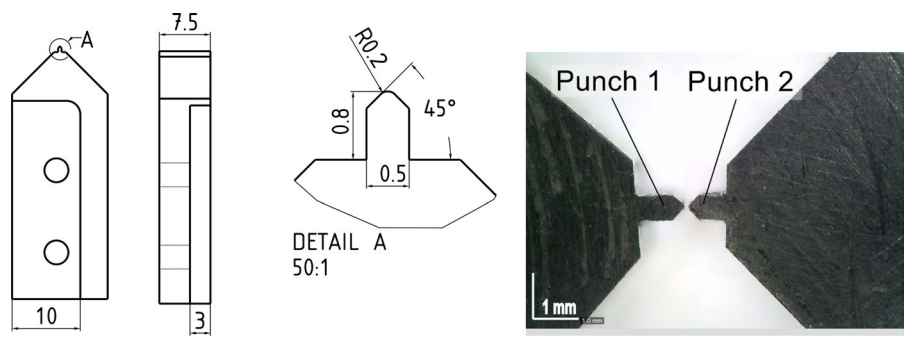

Fig. 2 Punches to form the FH notch: **a** punch geometry; **b** magnified representation of punches

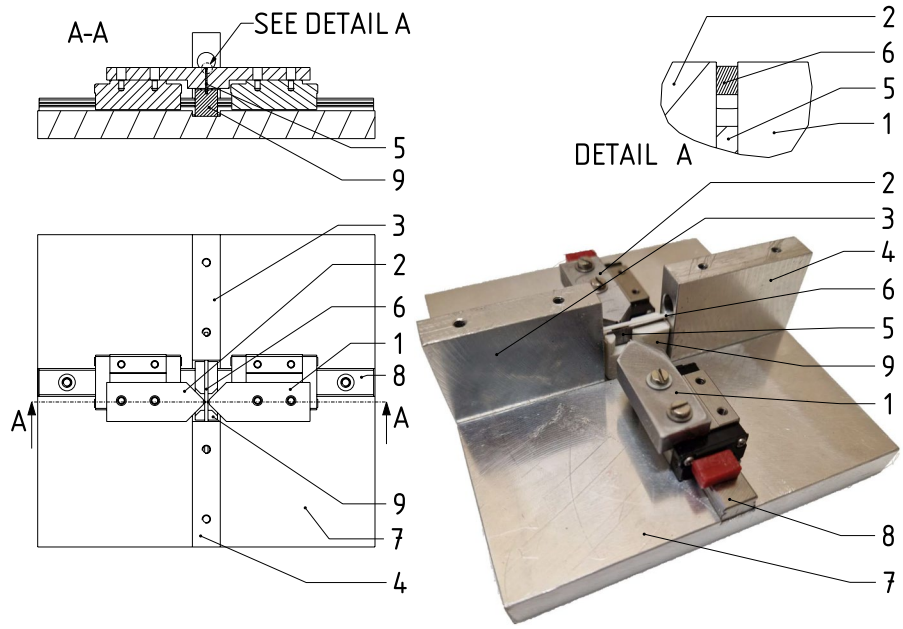

Fig. 3 Equipment for the plastic deformation of the 3D-PLAST process

shown in the figure). The whole unit is floating in the direction of the punch motion to ensure the punch-specimen ensemble's balance and the punching's symmetry.

2.5 3D-PLAST manufacturing process validation

Once all the specimens were manufactured, with both 3D printing and 3D-PLAST methods, they were tested by a bending endurance test. The testing was carried out manually using a specifically designed test rig (Fig. 4a). It features two plates which are assembled by screws and block one of the two rigid parts of the FH specimen, part F in Fig. 4b, while the other part, part M in Fig. 4b moves unrestrictedly in a plane orthogonal to the Z-axis of the specimen (Fig. 1b) within a conic slot obtained from the shape of the two plates once assembled together.

The device comprises three conical slots with 60°, 90°, and 120° vertex angles (2 α in Fig. 4b). The part F of the FH specimen is locked to the test rig in a position such that the movable part M can bend approximately about point O and lean against the inclined surfaces of the conical slot (see Fig. 4). The movable part M of the FH specimen is then moved back and forth within the conical slot, providing an alternate bending rotation α of ± 30°, ± 45°, ± 60°.

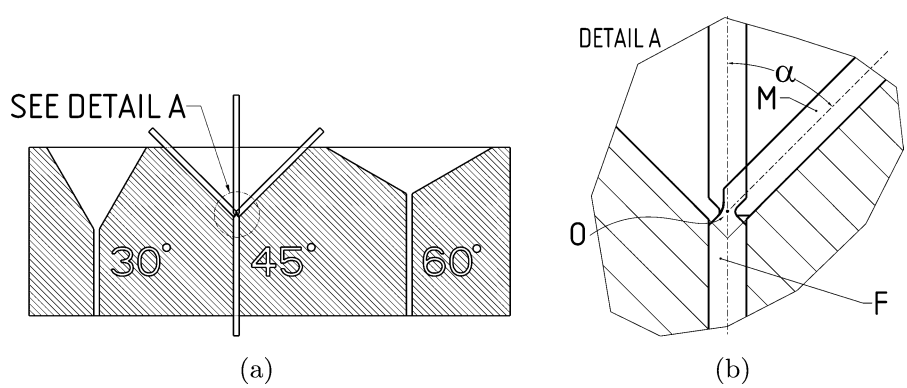

Fig. 4 Bending endurance FH test rig: **a** Test rig conical slots; **b** FH bending test

3 Results and discussion

A total of 88 specimens were produced: for Onyx, 21 were manufactured by 3D printing and 20 by 3D-Plast; for Nylon White, 20 by 3D printing and 27 for 3D-Plast. For each type, approximately half of the specimens were produced by mode 1 and the other by mode 2.

Results for the bending endurance test are reported in Fig. 5. Onyx 3D printed specimens failed, on average, before reaching 500 bending cycles over the three bending angles and two modes. The 3D-PLAST method increases the cycles up to 800. Instead, nylon made by the 3D printing method failed before 2000 cycles and for 3D-PLAST before 9000 cycles, although most specimens did not break at 9000 cycles. It is worth noting that the performance of the 3D-PLAST method specimens is better when the bending amplitude is ± 30°, where the cycles achieved are more than twice those achieved using the 3D printing method. A few tests, particularly those of the specimens made in Onyx with mode 2 with the alternate bending rotation of ± 45° and ± 60°, are not reported because they were influenced by incorrect loading conditions. In particular, the samples involved were subjected not only to alternating bending, but also to bending plus normal stress due to asymmetrical or incorrectly shaped flexure hinge geometry. In Fig. 6 examples of the FHs are reported that show the better quality of the FH shape obtained by the 3D-PLAST process (Fig. 6a) as compared to the final shape obtained only by the 3D printing process (Fig. 6b). More details could be observed by a deep analysis of the diagram reported in Fig. 5 where the Onyx specimens are shown on the left-hand side in a red-yellow set, and the Nylon specimens on the right-hand side, in a blue-light blue set. The abscissa shows the amplitudes of the alternate bending rotation, i.e.: ±30°, ±45° and ±60°. The different manufacturing modes (mode 1 and mode 2) are respectively at the left and right side of the demarcation vertical line in the centre of the same colour set. The ordinates show the number of cycles before failure of the specimen in a logarithmic scale. For each mode and bending angle amplitude, at least three specimens were tested, so each bar graph is made up of the best and worst result, and the average is indicated with a different coloured line within the bar. The results show that the proposed 3D-PLAST new process can significantly improve the life of the FHs.

To highlight the potentiality of the proposed method, an application example to a very well-known mechanism, i.e., the Cardan joint, has been realized. A 4 mm diameter Cardan with a hollow shaft with diameter of 1.7 mm, made of Onyx, has been designed and realized (see Fig. 7) by the new fabrication method presented in this paper. It has four bending hinges, that replaced the well known revolut

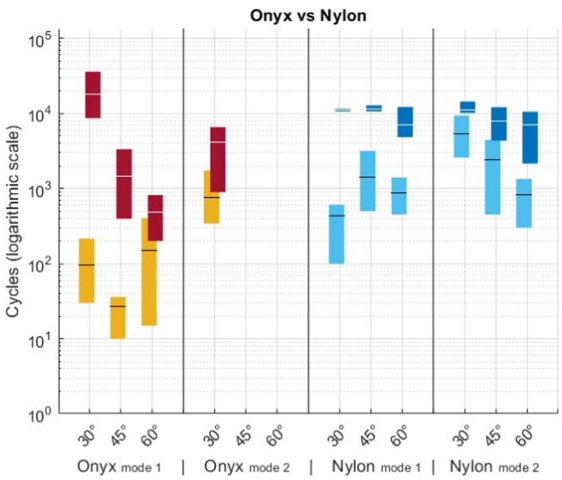

Fig. 5 Bending endurance test results. Onyx: 3D printing specimens (yellow); 3D-PLAST specimens (red). Nylon white: 3D printing specimens (light-blue); 3D-PLAST specimens (blue). Each set of colours is divided by a vertical demarcation line separating specimens made by mode 1 (left) from those made by mode 2 (right)

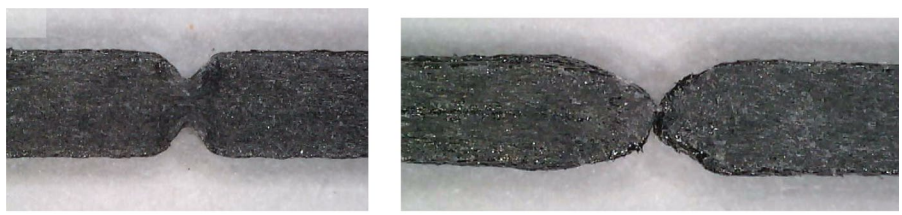

(a) (b)

Fig. 6 3D-PLAST versus 3D printing process: **a** 3D-PLAST FH; **b** 3D printing FH

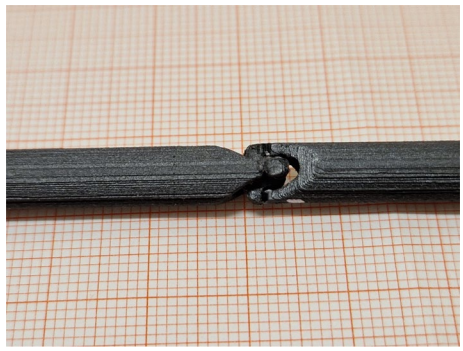

Fig. 7 A compliant Cardan joint obtained by the 3D-PLAST process

joints each at 90° apart from each other with axes on the same plane, arranged with the virtual rotation axes in the same plane and with the same dimensions and shapes as the hinges shown in this work. The Onyx material was chosen because the print result is more accurate and without unwanted cast material. A possible application can be, for instance, in laparoscopic devices [24], and its hollow part, also done in the Cardan cross, can leave room for additional functional transmission elements. For instance, it allows the introduction of a torsion cable of 1 mm diameter to control the opening and closing of the surgical tool. The complete mechanical characterization both in terms of kinematics and statics/stiffness characteristics of the Cardan joint is a subject of future work.

4 Conclusions

In this paper, the development and application of a novel fabrication method, named 3D-PLAST, have been explored to address the limitations faced by conventional additive manufacturing techniques in producing flexure hinges for compliant mechanisms, especially when the size of the filament is comparable with the FH's notch size, i.e., when the FH is very small.

The problem can be overcome by manufacturing the solid part of the system by the 3D printing method and then forming the FH by cold plastic deformation. Tests have been conducted on several FHs realized with different processes and materials, showing the effectiveness of the proposed 3D-PLAST method. Finally, a case study involving the fabrication of a 4 mm diameter Cardan hollow shaft illustrates 3D-PLAST's potential in crafting spatial mechanisms with enhanced functionality and precision. The proposed combined method is believed to have great potentiality in many compliant small devices, where traditional pairs proved to be less accurate, to guarantee low cost and accuracy not feasible with traditional joints.

Author Contributions All authors contributed equally to this work.

Funding Open access funding provided by Alma Mater Studiorum - Università di Bologna within the CRUI-CARE Agreement. The contribution of MUR through Next Generation EU - PNRR funding is gratefully acknowledged. The study has been co-funded by Tech Srl, Villanova di Castenaso (Bologna).

Data availability Detailed datasets are available upon request.

Declarations

Conflict of interest The authors declare no Conflict of interest.

Ethical approval Not applicable.

Open Access This article is licensed under a Creative Commons Attribution 4.0 International License, which permits use, sharing, adaptation, distribution and reproduction in any medium or format, as long as you give appropriate credit to the original author(s) and the source, provide a link to the Creative Commons licence, and indicate if changes were made. The images or other third party material in this article are included in the article's Creative Commons licence, unless indicated otherwise in a credit line to the material. If material is not included in the article's Creative Commons licence and your intended use is not permitted by statutory regulation or exceeds the permitted use, you will need to obtain permission directly from the copyright holder. To view a copy of this licence, visit http://creativecommons.org/licenses/by/4.0/.

References

1. Mutlu R, Alici G, In Het Panhuis M, Spinks G (2015) Effect of flexure hinge type on a 3d printed fully compliant prosthetic finger, 790–795 https://doi.org/10.1109/AIM.2015.7222634
2. Vyasarayani C, Birkett S, McPhee J (2009) Modeling the dynamics of a compliant piano action mechanism impacting an elastic stiff string. J Acoust Soc Am 125:4034–42. https://doi.org/10.1121/1.3125343
3. Lobontiu N (2002). Compliant mech: Des flexure hinges. https://doi.org/10.1201/9781420040272

4. Tian Y, Shirinzadeh B, Zhang D (2010) Closed-form compliance equations of filleted v-shaped flexure hinges for compliant mechanism design. Precis Eng 34:408–418. https://doi.org/10.1016/j.precisioneng.2009.10.002
5. Berselli G, Meng Q, Vertechy R, Parenti-Castelli V (2015) An improved design method for the dimensional synthesis of flexure-based compliant mechanisms: optimization procedure and experimental validation. Meccanica **51**(5) https://doi.org/10.1007/s11012-015-0276-z
6. Howell LL (2001) Compliant mechanisms. A Wiley-Interscience publication
7. Gouker RM, Gupta SK, Bruck HA, Holzschuh T (2006) Manufacturing of multi-material compliant mechanisms using multi-material molding. Int J Adv Manuf Tech 30:1049–1075. https://doi.org/10.1007/s00170-005-0152-4
8. Sieklicki W, Zoppi M, Molfino R (2009) Superelastic compliant mechanisms for needlescopic surgical wrists, 392–399
9. Guckenbergera DJ, De Groota TE, Wanb AMD, Beebea DJ, Young EWK (2015) Micromilling: A method for ultra-rapid prototyping of plastic microfluidic devices. Lab On A Chip 1:1–20. https://doi.org/10.1039/c0xx00000x
10. Radaelli G (2015) Modeling and design of origami mechanisms with compliant facets. Engineering Materials Science
11. Coemert S, Traeger MF, Graf EC, Lueth TC (2017) Suitability evaluation of various manufacturing technologies for the development of surgical snake-like manipulators from metals based on flexure hinges. Procedia CIRP 65:1–6. https://doi.org/10.1016/j.procir.2017.03.108
12. Culmone C, Smit G, Breedveld P (2019) Additive manufacturing of medical instruments: A state-of-the-art review. Addit Manuf 27:461–473. https://doi.org/10.1016/j.addma.2019.03.015
13. Krieger YS, Roppenecker DB, Stolzenburg J-U, Lueth TC (2016) First step towards an automated designed multi-arm snake-like robot for minimally invasive surgery. IEEE International Conference on Biomedical Robotics and Biomechatronics, 407–412 https://doi.org/10.1109/BIOROB.2016.7523661
14. Balderrama-Armendariz CO, MacDonald E, Roberson DA, Ruiz-Huerta L, Maldonado-Macias A, Valadez-Gutierrez E, Caballero-Ruiz A, Espalin D (2019) Folding behavior of thermoplastic hinges fabricated with polymer extrusion additive manufacturing. Int J Adv Manuf Tech 105:233–245. https://doi.org/10.1007/s00170-019-04196-x
15. Chun H, Guo X, Kim JS, Lee C (2020) A review: additive manufacturing of flexure mechanism for nanopositioning system. Int J Adv Manuf Tech 110(3):681–703. https://doi.org/10.1007/s00170-020-05757-1
16. Goodridge R, Ziegelmeier S (2016) Laser additive manufacturing: Powder bed fusion of polymers, 181–204 https://doi.org/10.1016/j.procir.2016.02.361
17. Gao W, Zhang Y, Ramanujan D, Ramani K, Chen Y, Williams CB, Wang CBL, Shin YC, Zhang S, D ZP (2015) The status, challenges, and future of additive manufacturing in engineering. Computer-Aided Design 69, 65–89 https://doi.org/10.1016/j.cad.2015.04.001.
18. Cuellar JS, Smit G, Plettenburg D, A Z (2018) Additive manufacturing of non-assembly mechanisms. Additive Manufacturing 21, 150–158 https://doi.org/10.1016/j.addma.2018.02.004
19. Lieneke, T., Denzer, V., A., A.G.O., D., Z.: (2016) Dimensional tolerances for additive manufacturing: Experimental investigation for fused deposition modeling. Procedia CIRP 43, 286–291 https://doi.org/10.1016/j.procir.2016.02.361
20. Polyzos E, Pyl L (2022) Effect of printing direction on the elastic properties of 3d-printed nylon materials. Phys Sci Forum 4(1):21. https://doi.org/10.3390/psf2022004021
21. Zou R, Xia Y, Liu S, Hu P, Hou W, Hu Q, Shan C (2016) Isotropic and anisotropic elasticity and yielding of 3d printed material. Compos Part B: Eng 99:506–513. https://doi.org/10.1016/j.compositesb.2016.06.009
22. Nikiema D, Balland P, Sergent A (2023) Study of the mechanical properties of 3d-printed onyx parts: Investigation on printing parameters and effect of humidity. Chinese Journal of Mechanical Engineering: Additive Manufacturing Frontiers **2**(2) https://doi.org/10.1016/j.cjmeam.2023.100075
23. Fisher T, Almeida Jr JHS, Falzon BG, Kazancı Z (2023) Tension and compression properties of 3d-printed composites: Print orientation and strain rate effects. Polymers **15**(7) https://doi.org/10.3390/polym15071708
24. Parenti-Castelli V, Manferrari F, Sancisi N, Vertechy R, Avallone G, Federici E, Battocchi F, Magnani L, Luzi L (2023) Laparoscopic surgical instrument. Patent application PTC/IT2020/000060, Pub.N.US2023/0285044A1

Publisher's Note Springer Nature remains neutral with regard to jurisdictional claims in published maps and institutional affiliations.